JOURNAL OF Materials CHEMISTRY

Study of fluorite phases in the system Bi_2O_3–Nb_2O_5–Ta_2O_5. Synthesis by mechanochemical activation assisted methods

Alicia Castro* and Damien Palem

Instituto de Ciencia de Materiales de Madrid, CSIC. Cantoblanco, 28049 Madrid, Spain. E-mail: acastro@icmm.csic.es

Received 19th April 2002, Accepted 17th June 2002
First published as an Advance Article on the web 30th July 2002

Mechanochemical activation followed by annealing at moderate temperatures results in the stabilisation, at room temperature, of different fluorite-type phases, belonging to the Bi_2O_3–Nb_2O_5, Bi_2O_3–Ta_2O_5 and Bi_2O_3–Nb_2O_5–Ta_2O_5 systems. The results obtained from different starting compositions and mechanical activation devices (vibrating and planetary ball mills) were compared with those obtained by classical solid-state synthesis methods. Vibrating ball mill activation yields amorphous precursors, which permits one to obtain fluorites with increasing pentavalent cation content when the annealing temperature is further increased. Planetary ball milling leads to the apparent mechanosynthesis of a fluorite phase at room temperature. The products were studied by X-ray powder diffraction at room temperature and above, thermal analysis techniques and transmission electron microscopy. Moreover, impedance spectroscopy measurements carried out on Bi_3MO_7 (M = Nb, Ta) fluorites, obtained by a mechanochemically assisted method, showed that these materials are good ionic conductors, with conductivities at 600 °C of 5×10^{-4} S cm^{-1} or higher, the processing history of the materials having a great influence on their properties.

Introduction

One of the best known solid-state oxygen-ion conductors is the high-temperature fluorite-type δ polymorph of Bi_2O_3.[1,2] Unfortunately, δ-Bi_2O_3 cannot be quenched to room temperature, but closely related phases can be isolated when doping with small quantities of numerous cations, preserving in most cases its good ionic conduction properties.[2–4]

The systems Bi_2O_3–Nb_2O_5 and Bi_2O_3–Ta_2O_5 have been extensively investigated over the entire range of composition.[5–7] The Bi_2O_3-rich ends of these systems have been shown to contain several single phases and solid solutions, all of them exhibiting fluorite-type superlattices.[8,9] Probably, the simplest compositions of these fluorites are of the type Bi_3MO_7 (M = Nb, Ta), where the niobium compound has shown very good conduction properties.[10,11]

In general, the synthesis of these materials is carried out *via* a conventional ceramic route that involves relatively high temperatures and long times of reaction, implying a possible problem of loss of stoichiometry, as well as the preparation of powdered samples with uncontrolled particle size. In order to avoid all these problems, mechanochemical activation synthesis of materials has become favoured in recent years. Various oxides have been prepared using mechanochemically-assisted methods for different applications, such as ferroelectric oxides,[12–14] ionic conductors,[15,16] cathode materials[17] or superconducting oxides.[18] A preliminary study on the preparation of fluorites derived from δ-Bi_2O_3, $(Bi_2O_3)_{0.75}(Y_2O_3)_{0.25}$ and $(Bi_2O_3)_{0.80}(Nb_2O_5)_{0.20}$, by mechanical alloying has been reported.[19,20]

This paper reports on the improvement of the synthesis conditions of fluorite phases belonging to the systems Bi_2O_3–M_2O_5 (M = Nb, Ta), and on the existence of a new solid solution $Bi_3Nb_{1-x}Ta_xO_7$ in the range of compositions, $0 \leqslant x \leqslant 1$. When mechanochemical activation methods are applied, the effect of varying the milling media, as well as the length of mechanical treatment and the temperature of annealing are discussed. The electrical behaviour of Bi_3NbO_7 and Bi_3TaO_7 single phases is studied by impedance spectroscopy.

Experimental

Two different procedures have been applied to synthesize Bi–Nb,Ta–O compounds: the classical solid-state reaction and mechanochemical activation methods. In the latter case, both vibrating and planetary mills were used. Stoichiometric mixtures of analytical grade Bi_2O_3 and Nb_2O_5 and/or Ta_2O_5, about 3 g in weight were initially homogenised by hand in an agate mortar. For the traditional ceramic route, the samples were subjected to increasing temperatures from 500 to 700 °C for 12 h each, with intermediate regrinding steps. For the mechanochemical activation, the Fritsch models Pulverisette 0 and 6 vibrating and planetary mills, respectively, were used. In both cases, the initial oxide mixture was placed in a stainless-steel pot with balls of the same material. In the vibrating mill a single ball of 5 cm diameter was used, whereas in the planetary mill, five balls of 1 cm diameter each were utilised, the grinding bowl being rotated at 260 rpm. In all cases the mechanochemical treatments were carried out in air, for times ranging from 1 to 360 h for the vibrating mill and from 1 to 87 h for the planetary mill. After treatment the powders were characterised by X-ray powder diffraction (XRD) at room and increasing temperatures, differential thermal analysis (DTA) and transmission electron microscopy (TEM).

Powder X-ray diffraction patterns were run at room temperature with a Siemens Kristalloflex 810 computer controlled diffractometer, and a D501 goniometer provided with a 2θ compensating slit and a graphite monochromator. Patterns were collected between 5 and 100° (2θ) with increments of 0.05° (2θ), counting time of 4 seconds per step; the goniometer was controlled by a DACO-MPV2 computer. To collect X-ray diffraction patterns at high temperature, an Anton Paar HTK10 attachment mounted on a Philips PW 1310 diffractometer was used between 5 and 70° (2θ) with increments of 0.02° (2θ) and counting times of 2 seconds per step. Each sample was deposited on a platinum sheet placed on a tantalum strip, which acts as the heating element. The temperature was measured using a Pt–Pt 13%Rh thermocouple welded onto the centre of the platinum sheet. The temperature was increased at a rate

 DOI: 10.1039/b203857a

of 10 °C min^{-1} and stabilised for the measurements. Cu-K_α (λ = 1.5418 Å) radiation was used in all experiments.

DTA curves were recorded up to 1000 °C on a Seiko 320 instrument at a heating rate of 10 °C min^{-1}. About 10 mg of sample was used for each run. Al_2O_3 was used as the reference material.

Dispersed particles of the milled powders were studied with a JEOL-2000FX TEM, working at 200 kV and equipped with energy dispersive spectroscopy (EDS) capability.

Electrical conductivity measurements were carried out by the complex impedance method in an 1174 Solartron frequency response analyser coupled to a 1286 Solartron electrochemical interface. Pellets of approximately 3 mm diameter and 1 mm thickness were prepared by cold pressing (1000 kg cm^{-2}) of a mechanically activated powder mixture. To form the phases, the pellets were heated at temperatures up to 800 °C, and slowly cooled to room temperature. This synthesis method was employed to improve the ceramic quality, as has been shown for other materials.[12,21] Platinum electrodes were deposited on the two faces by sputtering, and measurements were carried out in the temperature range 200–700 °C, at steady temperatures, with the pellets under air flow. The frequency range was 0.1–10^5 Hz.

Results and discussion

System Bi_2O_3–Nb_2O_5

Solid-state reactions between Bi_2O_3 and Nb_2O_5 have been carried out for comparative purposes, varying the Bi : Nb ratio between 4 : 1 and 1 : 1. As was previously reported,[10,11] the thermal treatment up to 700 °C leads to a single fluorite phase only for Bi : Nb = 3 : 1, corresponding to the Bi_3NbO_7 oxide. This fluorite crystallizes in the cubic system with unit-cell parameter 5.4788(9) Å, however it seems to represent the lower limit of the solid solution type II of the Bi_2O_3–Nb_2O_5 system, the higher limit being $Bi_{24}Nb_2O_{41}$.[22] According to our results, when Bi : Nb <3 a fluorite phase is obtained, together with other bismuth–niobium oxides like $Bi_5Nb_3O_{15}$ and $BiNbO_4$, whereas for Bi : Nb>3 the Bi_3NbO_7 fluorite can be obtained mixed with δ-Bi_2O_3. However, the unit-cell parameter calculated for each fluorite increases monotonically with increasing bismuth content, showing the existence of a solid solution near the Bi_3NbO_7 composition.

Two different starting compositions have been chosen to study the influence of the mechanochemical activation synthesis method on the synthesis of Bi_3NbO_7 fluorite: Bi_2O_3 : Nb_2O_5 = 3 : 1 and 2 : 1.

Table 1 summarizes the milling process and annealing conditions for the samples studied as well as the products identified. The X-ray diffraction patterns (XRD) of $3Bi_2O_3$: Nb_2O_5 sample milled in a vibrating ball mill for increasing times are compared in Fig. 1. For both compositions, the starting oxides progressively lose their crystalline characteristics with increasing grinding times. Initially, the XRD patterns display the whole set of peaks associated with the mixture of oxides. After a few hours these signals become significantly broadened and less intense, and when grinding proceeds for 120 h an amorphisation process sets in. Finally, after 144 and 360 h of milling only an amorphous phase is observed.

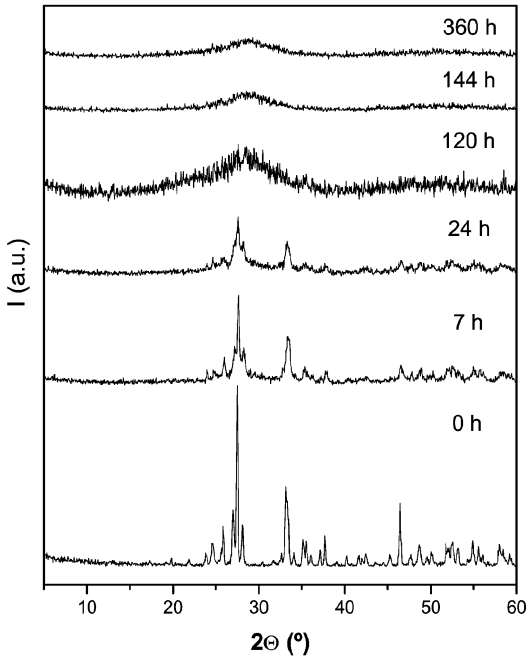

Fig. 1 XRD patterns taken at room temperature of a $3Bi_2O_3$: Nb_2O_5 oxide mixture, after different milling times in a vibrating ball mill.

In order to study the crystallization process of the fluorite phases the thermal behaviour of the amorphous phases (144 and 360 h milling for $3Bi_2O_3$: Nb_2O_5 and 360 h milling $2Bi_2O_3$: Nb_2O_5) were studied by both differential thermal analysis (DTA) and X-ray powder diffraction methods. As can be observed in Fig. 2, DTA curves of $3Bi_2O_3$: Nb_2O_5 activated samples show the existence of an irreversible exothermic process centred at about 300 °C, as well as another not well defined process at higher temperatures, particularly for the sample activated for 144 h. On the contrary, the DTA recording for the amorphous $2Bi_2O_3$: Nb_2O_5 sample exhibits two exothermic processes centred at 480 and 630 °C, respectively. Interpretation of DTA data was made on the basis of XRD taken at increasing temperatures (Fig. 3). In both $3Bi_2O_3$: Nb_2O_5 samples XRD confirms the presence of the amorphous material until the exothermic peak is observed at 300 °C, corresponding to the formation of a fluorite-type phase. This fluorite progressively evolves (diffraction line displacements) when temperature increases. Moreover, for the precursor activated for 144 h, some crystallization of the starting oxides can also be detected at 450 °C. The two exothermic processes observed for the $2Bi_2O_3$: Nb_2O_5 precursor are attributed to the crystallization of the fluorite phase and $Bi_5Nb_3O_{15}$ oxide,

Table 1 Milling times in the vibrating ball mill and annealing conditions for Bi_2O_3 : Nb_2O_5 = 3 : 1 and 2 : 1 and $3Bi_2O_3$: Ta_2O_5 samples, and resultant products (M = mixture of starting oxides; T = Ta_2O_5; A = amorphous; F = fluorite phase; B = $Bi_5Nb_3O_{15}$; t = trace)

	Milling times/h															
	$2Bi_2O_3$: Nb_2O_5						$3Bi_2O_3$: Nb_2O_5						$3Bi_2O_3$: Ta_2O_5			
Annealing temperature/°C	0	24	72	120	144	360	0	24	72	120	144	360	0	24	144	360
–	M	M	A+M	A+M_t	A	A	M	M+A	A+M	A	A	A	M	M+A	A+T	A+T
330	M	–	–	–	–	A	M	–	–	–	F+M	F	M	–	–	F
450	M	–	–	–	–	F	M	–	–	–	F+M	F	M	–	–	F
550	M	–	–	–	–	F+B	M	–	–	–	F+M	F	M	–	–	F
700	F+B	–	–	–	–	F+B	F	–	–	–	F	F	F	–	–	F

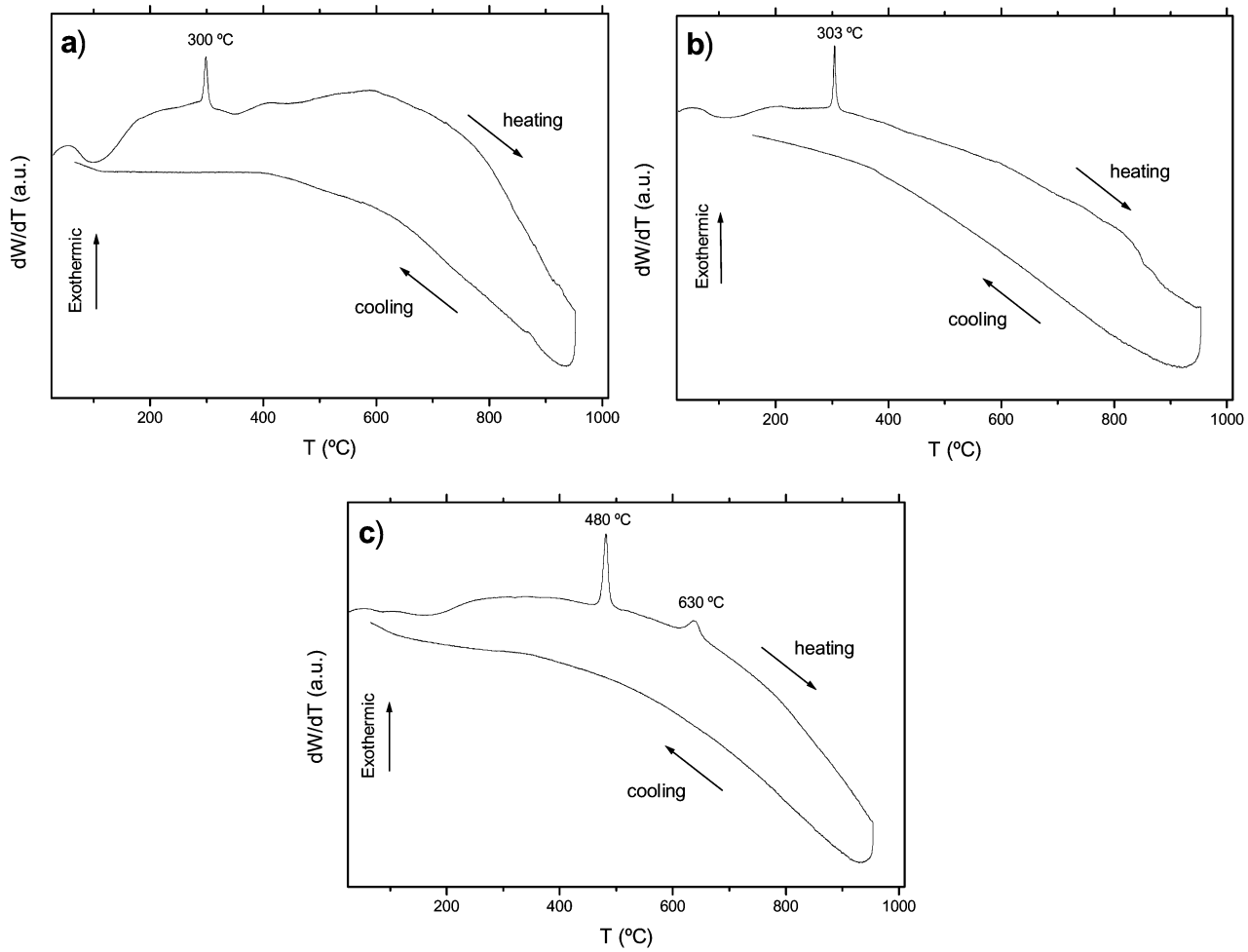

Fig. 2 Differential thermal analysis of amorphous powders after different lengths of milling time in a vibrating ball mill: a) $3Bi_2O_3$: Nb_2O_5, 144 h; b) $3Bi_2O_3$: Nb_2O_5, 360 h; and c) $2Bi_2O_3$: Nb_2O_5, 360 h.

respectively, in agreement with the results obtained through the traditional ceramic route.

To isolate each phase which is stable at room temperature, the precursors were heated in a furnace at temperatures similar to those used in the high-temperature XRD technique, and then quenched in air. The crystallographic transformations were analogous to those previously mentioned (Table 1). The unit-cell parameters calculated for the different fluorite phases are reported in Table 2. It is worth noting that the *a* parameter of the fluorites obtained at low temperature from the amorphous mechanoactivated precursors are greater than those of fluorites obtained at 700 °C, which is always the same for

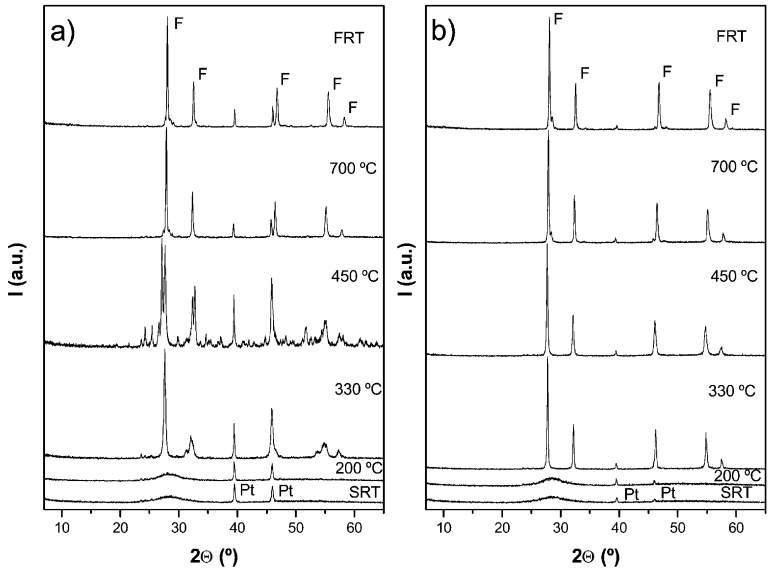

Fig. 3 X-Ray powder diffraction patterns at increasing temperatures of $3Bi_2O_3$: Nb_2O_5 amorphous powders from vibrating ball mill after different milling times: a) 144 h; and b) 360 h (Pt = platinum, F = fluorite phase, SRT = starting room temperature, FRT = final room temperature).

Table 2 Unit-cell parameters of fluorite-type phases obtained from different precursors at different annealing temperatures

Composition	Precursor	Annealing temperature/°C	a/Å
$3Bi_2O_3$: Nb_2O_5	Crystalline	700	5.4799(5)
	Amorphous, 360 h, vibrating	330	5.521(1)
		450	5.513(1)
		550	5.4829(5)
		700	5.4793(5)
	Fluorite, 5 h, planetary	280	5.517(1)
		450	5.504(1)
$2Bi_2O_3$: Nb_2O_5	Amorphous, 360 h, vibrating	480	5.445(1)
		700	5.465(2)
$3Bi_2O_3$: $0.75Nb_2O_5$: $0.25Ta_2O_5$	Crystalline	700	5.4799(5)
$3Bi_2O_3$: $0.5Nb_2O_5$: $0.5Ta_2O_5$	Crystalline	700	5.4780(5)
	Amorphous, 360 h, vibrating	360	5.487(1)
		700	5.4769(9)
$3Bi_2O_3$: $0.25Nb_2O_5$: $0.75Ta_2O_5$	Crystalline	700	5.477(1)
$3Bi_2O_3$: Ta_2O_5	Crystalline	700	5.4757(3)
	Amorphous 360 h vibrating	330	5.526(1)
		550	5.493(3)
		700	5.476(3)

$3Bi_2O_3$: Nb_2O_5 starting compositions, in agreement with the value reported for Bi_3NbO_7, synthesised by the solid-state reaction method. This fact must be due to the progressive incorporation of niobium atoms from the amorphous phase to the fluorite structure when the temperature increases, leading to the solid solution $Bi_3Nb_{1-\delta}O_{7-5\delta/2}$ (type II fluorite[8,9,22]), in such a way that the small Nb^{5+} cation substitutes for the larger Bi^{3+} ($r_{Nb}{}^{5+}$ = 0.74 Å, $r_{Bi}{}^{3+}$ = 1.17 Å[23]) in the host δ-Bi_2O_3 fluorite-type structure (a = 5.648 Å[24]). When the starting composition is rich in niobium ($2Bi_2O_3$: Nb_2O_5), the fluorite unit-cell parameters are lower at the same temperature, due to the higher niobium concentration, up to the limit temperature of 700 °C, where no single fluorite phase is attained.

In order to elucidate if some mechanosynthesis occurs during the mechanical treatment, a preliminary study by TEM of the $3Bi_2O_3$: Nb_2O_5 powder activated for 360 h has been carried out (Fig. 4). Electron diffraction measurements confirm that the majority of particles are amorphous, although some crystalline particles can also be observed. The amorphous particles show sizes between 200 and 300 nm, while the crystalline ones are around 50 nm. The small size of these crystallites causes a line broadening effect in the X-ray diffraction pattern, which together with the fact that only small quantities are observed, makes them practically undetectable. EDS analysis of a large amount of these particles shows that most crystalline particles are rich in niobium and those which are amorphous are rich in bismuth. Only a few amorphous particles exhibit the Bi : Nb ratio 3 : 1. So, if we consider that amorphous particles are highly reactive,[25] the absence of amorphous particles from one of the starting oxides (Nb_2O_5) may prevent mechanosynthesis from taking place.

The results obtained by mechanochemical activation of $3Bi_2O_3$: Nb_2O_5 in a planetary mill are shown in Fig. 5. The behaviour observed is different from that of the vibrating mill treatment. Here the diffraction lines of the starting oxides broadened in a very short time, about 30 minutes, then a pattern reminiscent of a fluorite structure developed, and it remained as the only crystalline phase detected after 5 hours of mechanical treatment. It could be said that the observations are compatible with a process of mechanosynthesis, even if this

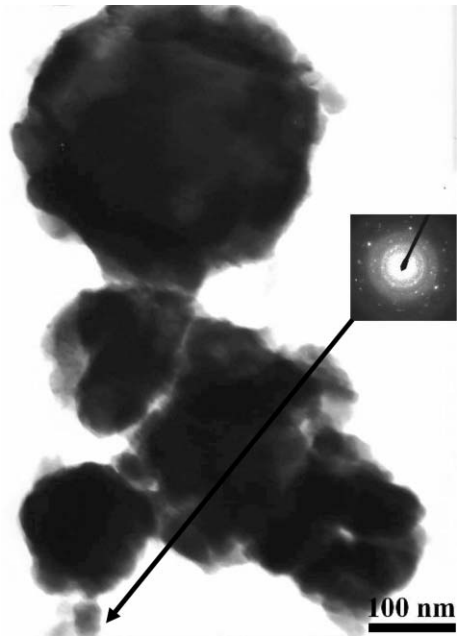

Fig. 4 TEM micrograph of several particles from the $3Bi_2O_3$: Nb_2O_5 mixture mechanoactivated for 360 h. The larger particles are identified as amorphous by electron diffraction. The smaller particle marked with an arrow is crystalline (inset the corresponding electron diffraction pattern).

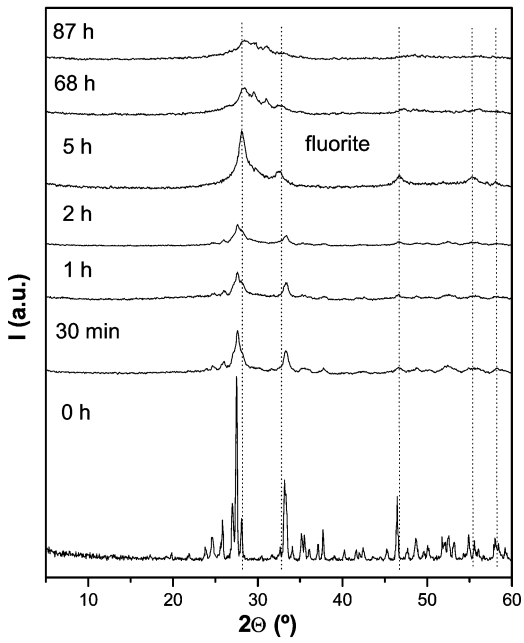

Fig. 5 X-Ray pattern evolution of a $3Bi_2O_3$: Nb_2O_5 mixture with milling time in a planetary ball mill.

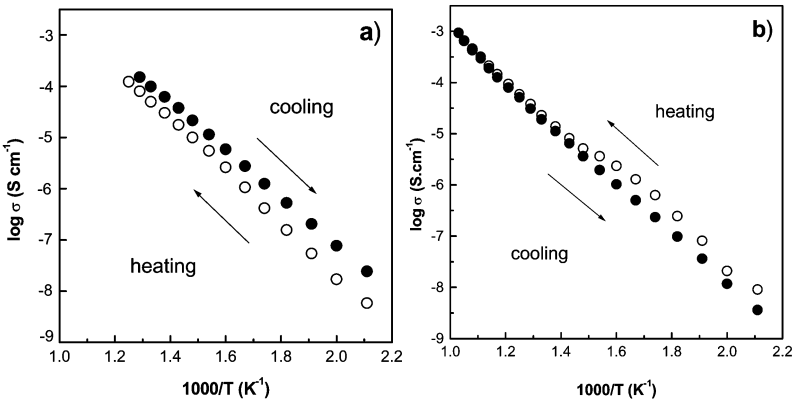

Fig. 6 Arrhenius plots of conductivity for a) Bi_3NbO_7 and b) Bi_3TaO_7, materials obtained by mechanochemically-assisted synthesis method.

mechanosynthesis is not complete. Further milling led to an almost amorphous phase.

The thermal behaviour of both mechanosynthesized fluorite (5 h milling) and amorphous phase (87 h milling) was studied. DTA curves show the existence of an exothermic process centred at temperatures that increase when the period of the mechanical treatment is increased. According to the XRD data, this process corresponds to the crystallization of different fluorites, that can only be isolated as a single phase (Table 2) by low temperature treatments of the apparently mechanosynthesized fluorite. On the contrary, treatments at temperatures higher than 450 °C, or even at low temperature for the case of the amorphous product milled for 87 h, led to a mixture of a fluorite phase and $BiNbO_4$.

These results permit one to conclude that the mechanical treatment in a planetary mill is too drastic, giving rise to the mechanosynthesis of a fluorite phase, but also to other secondary mixed oxides that can crystallize at moderate temperatures. Therefore, mechanochemical activation in a vibrating mill seems preferable for the isolation of single fluorite phases in the system Bi_2O_3–Nb_2O_5.

Finally, the oxide ion conduction of the so stabilized Bi_3NbO_7 material was studied. For this purpose, pellets of this material were prepared from a precursor vibrating milled for 144 h, according to the conditions described in the Experimental section. The conductivity (log σ) as a function of inverse temperature (1000/T) is depicted in Fig. 6a. The experimental data are well fitted to the Arrhenius expression $\sigma = \sigma_0 \exp(-E_a/kT)$ where σ_0 is a pre-exponential factor, E_a the activation energy and k the Boltzmann constant. The electrical conductivities on heating and cooling are quite similar, with activation energies of 1.01 eV on heating and 0.91 eV on cooling, the highest conductivity measured being 5×10^{-4} S cm^{-1} at 600 °C. The different σ values found in the heating and cooling runs could be related to a new sintering process occurring during the measurement cycle. It is difficult to compare this result with the maximum conductivity reported ($\sigma = 4.2 \times 10^{-4}$ S cm^{-1} at 500 °C[10]) for Bi_3NbO_7 obtained by solid-state reaction, because the processing conditions of the materials were different, with higher pressure and heating temperature in the latter case. In general, a main factor to improve the conductivity response of a material is to increase the sintering temperature of the pellets, as has been proved in the γ-$Bi_2V_{0.9}Cu_{0.1}O_{5.5}$ phase,[26] for example, which represents one of the best oxide ion conductors known. In our case, quite good properties are obtained following a simplified synthesis and processing method.

System Bi_2O_3–Ta_2O_5

A similar study to that above mentioned for the Bi_2O_3–Nb_2O_5 system was made for the system Bi_2O_3–Ta_2O_5 as well. In this case, only the starting composition $3Bi_2O_3$: Ta_2O_5 was considered, taking into account the better results obtained for this composition in the niobium system.

The existence of the Bi_3TaO_7 fluorite is also well known, representing the lower limit of the so-called type II solid solution Bi_3TaO_7–Bi_9TaO_{16}.[8,9] The results obtained in the present work, when the synthesis was carried out by the traditional ceramic route with Bi_2O_3 and Ta_2O_5, agree with those reported by other authors,[27] who obtained the single fluorite phase Bi_3TaO_7 after heating at 700 °C or higher.

The mechanochemical activation of $3Bi_2O_3$: Ta_2O_5 was also carried out using both vibrating and planetary ball mills. The evolution of the XRD patterns with milling time is shown in Fig. 7a (vibrating mill) and Fig. 7b (planetary mill). As occurs for the $3Bi_2O_3$: Nb_2O_5 system, a progressive broadening of the diffraction lines is observed with increasing milling time in the vibrating mill, but the main difference observed in the present case is that no amorphous phase was obtained after long mechanical treatment (360 h), but instead some crystalline Ta_2O_5 was always obtained (Table 1). In the planetary mill the tantalum oxide remains also a crystalline phase up to 5 h of mechanical treatment, together with a fluorite-type structure that was mechanosynthesized. Mechanical treatments as long as 40 h were needed to obtain the fluorite phase without the presence of crystalline Ta_2O_5. In summary, the main difference for the mechanochemical activation of $3Bi_2O_3$: Nb_2O_5 and $3Bi_2O_3$: Ta_2O_5 mixture of oxides can be found in the behaviour of the M_2O_5 oxides, for which longer and very energetic mechanical treatments are essential to damage the structure of the tantalum oxide and activate it.

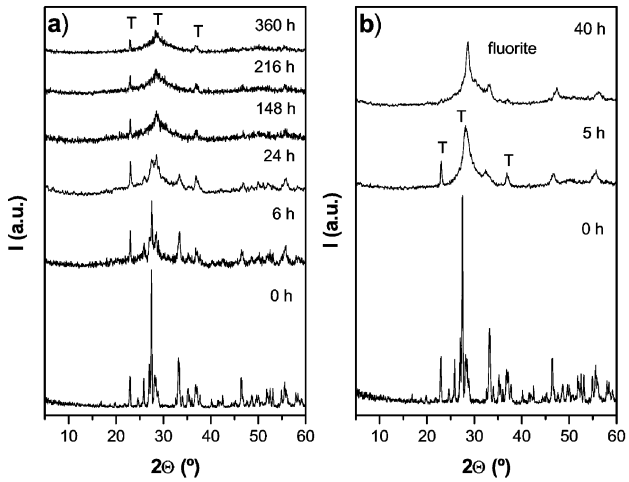

Fig. 7 X-Ray diffraction patterns of a $3Bi_2O_3$: Ta_2O_5 mixture of oxides mechanochemically activated in a) a vibrating ball mill; b) a planetary ball mill (T = Ta_2O_5).

The thermal behaviour of the mechanoactivated precursors of the $3Bi_2O_3$: Ta_2O_5 composition was very similar to that of $3Bi_2O_3$: Nb_2O_5. DTA curves (data not shown) exhibit exothermic irreversible transitions occurring at different temperatures, related to the crystallization of different fluorite phases. The unit-cell parameter values of the fluorites obtained by annealing of the amorphous activated precursor (360 h milling in vibrating ball mill) are reported in Table 2. The diminution of the *a* parameter with increasing annealing temperature is in agreement with the results found for the $3Bi_2O_3$: Nb_2O_5 precursor. As in that case, this evolution can be explained as being due to the progressive incorporation of tantalum cations to the δ-Bi_2O_3 fluorite framework. Again, the annealing of the precursor activated for 40 h in the planetary mill does not lead to the synthesis of single fluorite phases, but these are obtained mixed with several Bi–Ta oxides.

A study of the electrical conductivity was performed on the Bi_3TaO_7 material, processed from the precursor vibrating mill activated for 360 h. Experimental conductivity values were fitted to an Arrhenius plot (Fig. 6b). From the plot in the heating run it is possible to draw two slopes: one between 200 and 400 °C and the other in the interval 400 to 700 °C. This change of slope does not correspond to a structural transition, but could be attributed to a compositional change, the high temperature phase being the richest in tantalum. On the cooling run, a unique straight line is observed, coincident with the high temperature line obtained on heating, so it can be concluded that no further transition takes place. The energy activation calculated from the cooling data is very close to 1 eV, and the maximum conductivity reached is $\approx 7 \times 10^{-4}$ S cm^{-1} at 700 °C, with a similar behaviour to the Bi_3NbO_7 fluorite.

System Bi_2O_3–Nb_2O_5–Ta_2O_5

In order to verify the existence of a continuous solid solution between Bi_3TaO_7 and Bi_3NbO_7 fluorites, three compositions $3Bi_2O_3$: $(1-x)Nb_2O_5$: xTa_2O_5, $x = 0.25$, 0.5 and 0.75, have been treated at increasing temperatures between 500 and 700 °C. In all cases, $Bi_3Nb_{1-x}Ta_xO_7$ fluorite-type single phases were obtained by the solid-state reaction method. The unit-cell parameters of these new fluorite oxides are reported in Table 2. As can be observed, the *a* value diminishes monotonically with tantalum content. This fact cannot be attributed to the ionic radii of Nb^{5+} and Ta^{5+} cations because they have the same value (0.74 Å[23]), but to the higher polarizing power of the Ta^{5+} cation, that leads to a higher covalent contribution to the Ta–O bond, and then to the observed slight evolution of the fluorite framework.[28]

The mechanochemically-assisted synthesis method, using a vibrating ball mill, has been carried out for the intermediate stoichiometry $3Bi_2O_3$: $0.5Nb_2O_5$: $0.5Ta_2O_5$, as a representative composition of the solid solution. After 360 hours of mechanical treatment, an almost amorphous sample is obtained, but a small quantity of crystalline Ta_2O_5 oxide was still detectable by XRD. This result is in perfect agreement with those obtained for the limit compositions $3Bi_2O_3$: Nb_2O_5 and $3Bi_2O_3$: Ta_2O_5.

The DTA curve of this precursor shows a unique exothermic effect on heating, centred at 360 °C, that should be due to the crystallisation of a fluorite phase. Thermal annealing at increasing temperatures has been carried out in a furnace obtaining, as in the previous cases, fluorite phases with unit-cell parameters that decrease with increasing temperatures. Again, this fact is correlated to the progressive incorporation of pentavalent cations into the fluorite framework; probably Nb^{5+} can be easily incorporated because it is more activated, while Ta^{5+} partially remains as crystalline Ta_2O_5.

Conclusions

A new solid solution $Bi_3Nb_{1-x}Ta_xO_7$ has been obtained by solid-state reaction methods. The structural characteristics of these materials are intermediate between the niobium, Bi_3NbO_7, and tantalum, Bi_3TaO_7, phases, exhibiting a diminution of unit-cell parameters with increasing tantalum content. This fact is attributed to the higher polarizing power of the Ta^{5+} cation.

The mechanochemically-assisted synthesis has been revealed to be a useful method to isolate different fluorite phases in the systems studied. The planetary ball mill seems to supply more energy to the reactants, and produces the apparent mechanosynthesis of fluorite-type oxides in short mechanical treatment times. However, the vibrating ball mill leads to the amorphisation of the starting products, and no mechanosynthesis can be detected.

Further thermal annealing of the mechanoactivated precursors permits one to isolate different crystalline fluorite phases, with larger unit-cell parameters for lower temperature treatments. This fact could be attributed to the progressive incorporation of niobium and/or tantalum into the δ-Bi_2O_3 host fluorite framework.

Both Bi_3MO_7 (M = Nb, Ta) are good ionic conductors, with maximum conductivities of 5×10^{-4} S cm^{-1} or higher at 600 °C. The electrical behaviour of these materials is closely related to the processing methods followed to obtain them.

Acknowledgements

The authors thank Professor J. E. Iglesias for many valuable discussions, and Dr J. M. Rojo and Dr J. Ricote for assistance with impedance and TEM measurements, respectively. The financial support of the MCYT of Spain (project MAT2001-0561) is gratefully acknowledged.

References

1 T. Takahashi and H. Iwahara, *Mater. Res. Bull.*, 1978, **13**, 1447.
2 E. C. Subbarao and H. S. Maiti, *Solid State Ionics*, 1984, **11**, 317.
3 H. T. Cahen, T. G. M. van den Bett, J. H. W. de With and G. H. J. Broers, *Solid State Ionics*, 1980, **1**, 411.
4 H. Iwahara, T. Esaka, T. Sato and T. Takahashi, *J. Solid State Chem.*, 1981, **39**, 173.
5 R. S. Roth and T. L. Waring, *J. Res. Natl. Bur. Stand., Sect. A*, 1962, **66**, 451.
6 W. Zhou, D. A. Jefferson, M. Alario-Franco and J. M. Thomas, *J. Phys. Chem.*, 1987, **91**, 512.
7 R. Mida and M. Tanaka, *Jpn. J. Appl. Phys.*, 1990, **29**, 1132.
8 C. D. Ling, R. L. Withers, S. Schmid and J. G. Thompson, *J. Solid State Chem.*, 1998, **137**, 42.
9 C. D. Ling, *J. Solid State Chem.*, 1999, **148**, 380.
10 A. Castro, E. Aguado, J. M. Rojo, P. Herrero, R. Enjalbert and J. Galy, *Mater. Res. Bull.*, 1998, **33**, 31.
11 E. Aguado, R. Enjalbert, J. M. Rojo and A. Castro, *Bol. Soc. Esp. Ceram. Vidrio*, 1995, **34**, 417.
12 A. Castro, P. Millán, L. Pardo and B. Jiménez, *J. Mater. Chem.*, 1999, **9**, 1313.
13 J. G. Lisoni, P. Millán, E. Vila, J. L. Martín de Vidales, Th. Hoffmann and A. Castro, *Chem. Mater.*, 2001, **13**, 2084.
14 L. B. Kong, J. Ma, W. Zhu and O. K. Tan, *Mater. Res. Bull.*, 2002, **37**, 23.
15 A. Castro, P. Millán, J. Ricote and L. Pardo, *J. Mater. Chem.*, 2000, **10**, 767.
16 K. Shantha, G. N. Subbanna and K. B. R. Varma, *J. Solid State Chem.*, 1999, **142**, 41.
17 W. T. Jeong and K. S. Lee, *J. Alloys. Compd.*, 2001, **322**, 205.
18 J. M. González-Calbet, J. Alonso, E. Herrero and M. Vallet-Regí, *Solid State Ionics*, 1997, **101**(103), 119.
19 T. Esaka, S. Takai and N. Nishimura, *Denki Kagaku*, 1996, **64**, 1012.
20 S. Takai, N. Nishimura, T. Atake and T. Esaka, *Electrochemistry*, 1999, **67**, 466.
21 L. Pardo, A. Castro, P. Millán, C. Alemany, R. Jiménez and B. Jiménez, *Acta Mater.*, 2000, **48**, 2421.

22 W. Zhou, *J. Solid State Chem.*, 2002, **163**, 479.
23 R. D. Shannon, *Acta Crystallogr., Sect. A*, 1976, **32**, 751.
24 P. D. Battle, C. R. A. Catlow, J. Drennan and A. D. Murray, *J. Phys. C: Solid State Phys.*, 1983, **16**, L561.
25 J. Ricote, L. Pardo, A. Castro and P. Millán, *J. Solid State Chem.*, 2001, **160**, 54.
26 K. Reiselhuber, G. Dorner and M. W. Breiter, *Electrochim. Acta*, 1993, **38**, 969.
27 W. Zhou, *J. Solid State Chem.*, 1992, **101**, 1.
28 A. F. Wells, in *Structural Inorganic Chemistry*, Clarendon Press, Oxford, 5th edn., 1984.